Food cannery effluent, pineapple peel as an effective low-cost biosorbent for removing cationic dye from aqueous solutions

R.R. Krishni[a], K.Y. Foo[b], B.H. Hameed[a],*

[a]School of Chemical Engineering, Engineering Campus, Universiti Sains Malaysia, 14300 Nibong Tebal, Malaysia
Tel. +604 5996422; Fax: +604 5941013; email: chbassim@eng.usm.my
[b]Environment and Occupational Health Programme, School of Health Sciences, Health Campus,
Universiti Sains Malaysia, 16150 Kubang Kerian, Malaysia

ABSTRACT

The present research explores the viability of pineapple peel, an agricultural effluent discharged from the food can processing industries for removing methylene blue (MB) dye from the aqueous solution. The effects of contact time, initial concentration, and solution pH on the adsorptive uptake of MB were investigated in a batch mode study. The morphological and functional characterization of the adsorbent was performed using the scanning electron microscopy and Fourier transform infrared analysis. The adsorption equilibrium was simulated using the Langmuir, Freundlich and Temkin isotherm models. Kinetic modeling was fitted to the pseudo-first-order and pseudo-second-order kinetic equations, while the adsorption mechanism was determined using the intraparticle diffusion model. Equilibrium data were favorably described by the Langmuir isotherm model, with a maximum monolayer adsorption capacity of 97.09 mg/g. The results provide a strong evidence to support the potential use of pineapple waste as an effective adsorbent for the treatment of textile wastewater.

Keywords: Adsorption; Isotherm; Kinetic; Methylene blue; Pineapple peel

1. Introduction

Water scarcity and air pollution rank equal to climate change as the most intricate environmental turmoil for the twenty-first century. Today, rapidly changing technologies, industrial products and practices generate waste that if improperly managed, could threaten public health and the environment [1]. Various industries such as dye manufacturing, pulp and paper tanneries, cosmetic, coffee pulping, pharmaceuticals, food processing, electroplating and distilleries spew out colored and toxic effluents to water bodies rendering them murky, dirty and unusable for further use. Among different pollutants of aquatic ecosystems, dyes are a large and important group of industrial chemicals with over 700,000 tons of waste produced annually [2]. Statistically, the total dye consumption of the textile industry is in excess of 10^7 kg/y, and an estimated 90% of this ends up on fabrics [3].

Numerous studies have been conducted to assess the harm impacts of colorants on the ecosystem. The real hazard setting aside esthetic considerations is caused when these colored agents interfere with the transmission of light through water, retard

*Corresponding author.

photosynthetic activities in the aquatic life, and damage the quality of the receiving streams and food chain equilibrium [4]. Acute exposure to colored effluents may cause shock, Heinz body formation, cyanosis, jaundice, quadriplegia, tissue necrosis, allergy, dermatitis, irritation and present carcinogenic and mutagenic effects [5,6].

Over the years, a wide range of conventional treatment technologies for dye removal has been investigated extensively. The conventional methods for treating dye-containing wastewater include coagulation/flocculation, sedimentation, membrane technologies, cloud point extraction, microbiological decomposition, biological degradation, electrochemical treatment, and adsorbent utilization [7–16]. In particular, activated carbon adsorption process has been found to be superior to other techniques, in terms of its simplicity of design, ease of operation, insensitivity to toxic substances and complete removal of dyes, even from dilute solutions [17]. Despite its prolific use in wastewater treatment, the biggest barrier of the application by the industries is the cost-prohibitive adsorbent and difficulties associated with regeneration [18]. This has prompted to a growing research interest to establish the reliability of natural, renewable, and low-cost materials as alternative adsorbents for water pollution control.

In this respect, pineapple (*Ananas comosus* Merr.), is a herbaceous perennial plant native to Paraguay and the southern part of Brazil, with a height of 1.0–1.5 m. The fruits are arranged in two interlocking helices, eight in one direction, thirteen in the other, each being a Fibonacci number [19]. Pineapple is primarily eaten fresh and available as food complements in desserts, salads, fruit cocktail, jam, juice combinations or can food processing industries [20]. However, the wide-scale implementations in the food manufacturing industries are deteriorated by the massive generation of leaves and stems waste, which constitutes 30% of the entire fruit. The focus of this study was intended to evaluate the adsorption potential of waste pineapple leaves collected from the food can processing industries for removing methylene blue (MB) dye from the aqueous solutions. Textural and functional characterization of the prepared adsorbent was performed. Moreover, the effect of initial dye concentration, contact time, solution pH, adsorption isotherm, kinetics, and mechanism are outlined.

2. Materials and methods

2.1. Adsorbate

Methylene blue, an analytical grade cationic dye purchased from Sigma-Aldrich (M) Sdn. Bhd,

Malaysia was chosen as the targeted adsorbate in this study. Deionized water supplied by USF ELGA water treatment system was used to prepare all the reagents and solutions.

2.2. Preparation and characterization of adsorbent

Pineapple leaves required for the preparation of adsorbent were collected from a local food can processing factory. The precursor was washed thoroughly with distilled water to remove adhered impurities from its surface. Then, it was cut into small pieces (1–3 cm) and dried in an oven at 70°C for 48 h. The dried sample was screened to a fraction of 355–500 μm, repeatedly washed with hot distilled water, and dried overnight at 70°C. No physical or chemical treatments were performed prior to the adsorption experiments. Scanning electron microscopy (SEM) analysis (Zeiss Supra 35 VP) was carried out to study the surface texture of adsorbent before and after the adsorption of MB. Fourier transform infrared (FTIR) spectroscopy (FTIR-2000, PerkinElmer) was applied to determine the surface functional groups of the prepared adsorbent from the scanning range of 4,000–400 cm^{-1}.

2.3. Batch adsorption studies

The batch adsorption studies were conducted in a set of 250-mL Erlenmeyer flasks containing 0.30 g of adsorbent and 200 mL of MB solutions with the concentrations 50–300 mg/L. The flasks were agitated in an isothermal water bath shaker at 120 rpm and 30°C until the equilibrium was achieved. All samples were filtered prior to analysis to minimize the interference of adsorbent fines with the analysis. The concentrations of MB in the supernatant solutions before and after the adsorption of MB were analyzed using a double-beam UV–vis spectrophotometer (Shimadzu UV-1601, Japan) at 668 nm. Each experiment was duplicated under identical conditions. MB uptake at equilibrium, q_e (mg/g), was calculated by the following:

$$q_e = \frac{(C_o - C_e)V}{W} \tag{1}$$

where C_0 and C_e (mg/L) are the liquid-phase concentrations of MB solution at initial and equilibrium, respectively. V is the volume of the solution (L), and W is the mass of adsorbent used (g).

2.4. Effect of solution pH

The effect of solution pH on the adsorptive uptake of MB was examined by varying the initial pH from

pH 2 to 10, at the fixed adsorbent dosage of 0.30 g/200 mL, initial dye concentration of 200 mg/L, and adsorption temperature of 30℃. The pH was adjusted using the 0.1 M HCl or NaOH solutions.

2.5. Adsorption kinetic studies

For interpretation of adsorption kinetics, the aqueous samples were withdrawn at different time intervals and the concentrations of MB were similarly measured. The amount of adsorption at time t, q_t (mg/g), was calculated by:

$$q_t = \frac{(C_o - C_t)V}{W} \tag{2}$$

where C_t (mg/l) is the liquid-phase concentration of dye at time, t.

3. Results and discussions

3.1. Effect of initial concentration and contact time on the adsorption of MB

The effect of initial concentration and contact time on the adsorption of MB is depicted in Fig. 1. Generally, the plots can be divided into three distinct regions: (1) rapid adsorption during the first 20 min, (2) gradual equilibrium till the equilibrium state, and (3) a plateau. At this point, the amount of dye desorbing from the adsorbent is in a state of dynamic equilibrium with the amount of dye being adsorbed onto the adsorbent. The time required to attain this state of equilibrium is termed as equilibrium time, and the amount of dye adsorbed at the equilibrium reflected the maximum adsorption capacity of the adsorbent under those operating conditions [21,22]. The result is attributed to the fact that a large number of vacant surface sites are available at the initial stage, and after

a lapse of time, the remaining vacant surface sites are difficult to be occupied due to repulsive forces between the solute molecules on the solid and bulk phases. Similar trend was observed in the adsorption of MB onto Shaddock peel and clay particles [23,24].

Initial concentration provides a driving force to overcome mass transfer resistances of dye molecules between aqueous solution and the solid medium. In the present study, the adsorption equilibrium of MB, q_e increased from 31.81 to 94.97 mg/g with increasing the initial concentration from 50 to 300 mg/L. This process took relatively longer contact time and the time profile of dye uptake is a single, smooth and continuous curve leading to saturation, suggesting possible monolayer coverage of dye onto the surface of adsorbent. At lower concentrations of 50 mg/L, full equilibrium was attained in less than 120 min. However, at higher concentration of 100–300 mg/L, a relatively longer contact time ranged between 240 and 280 min was required for MB solutions to reach to the equilibrium. Similar observation was reported for the adsorption of MB onto lotus leaf and natural zeolite [25,26]. This illustrates that the adsorption performance of the prepared adsorbent was comparable with the works carried out by previous researchers.

3.2. Effect of solution pH on dye adsorption

Fig. 2 shows the effect of solution pH on the adsorptive uptake of MB. The adsorptive uptake of MB increased from 11.29 to 107.00 mg/g with increasing the solution pH from 2 to 12. The maximum q_e was observed at pH 6 where no significant changes were noticed beyond the value. This behavior is associated with the presence of excess H$^+$ ions, which present a competitive impact with dye molecules for the adsorption sites. Besides lower solution pH also induces the protonation of MB in the acidic medium and development of positive charge onto the
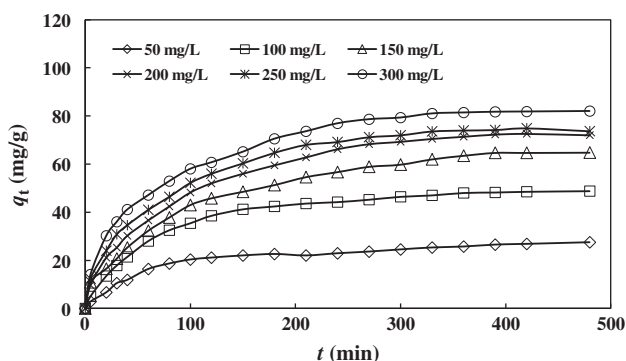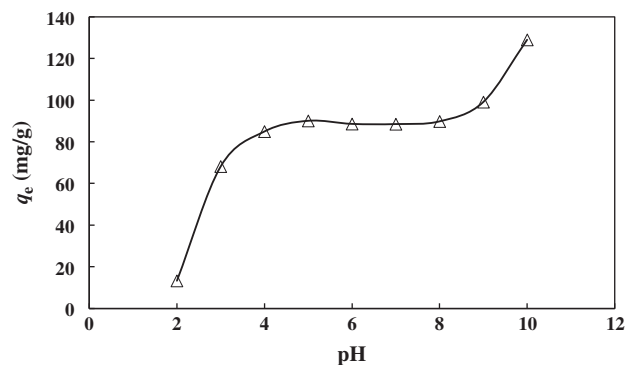

Fig. 1. Effect of initial concentration on the adsorptive uptake of MB by pineapple leaves derived adsorbent (conditions: $W = 0.30$ g/200 mL; temperature = 30℃).

Fig. 2. Effect of solution pH on the adsorption uptake of MB ($C_0 = 250$ mg/L, temperature 30℃ and $W = 0.30$ g).

adsorbent surface, which inhibits the accessibility of the pores structure [27]. However, in the basic medium, the formation of electric double layer changes its polarity, and consequently dye uptake increases. The result is in good agreements with the previous findings [28,29].

3.3. Adsorption isotherms

Adsorption isotherms reveal the specific relation between adsorbate concentration in the bulk and adsorbed amount at the interface [30]. Therefore, in the present study, three common isotherm models were established, namely the Freundlich, Langmuir and Temkin isotherm models. The applicability of the isotherm equation was compared by judging the correlation coefficients, R^2.

Freundlich isotherm [31] is the earliest known relationship describing the adsorption process. It endorses the heterogeneity of surface, with different binding energy. The empirical model is generally suitable for high and middle-concentration environments but is not suitable for low concentrations because it does not meet with the requirements of Henry's law. The linear form of Freundlich isotherm is expressed as follows:

$$\log q_e = \log K_F + \frac{1}{n}\log C_e \tag{3}$$

where K_F (mg/g (l/mg)1/n) and n are Freundlich constants related to adsorption capacity and adsorption intensity of the adsorbent. K_F can be defined as the adsorption coefficient and represents the quantity of dye adsorbed onto adsorbent for a unit equilibrium concentration. Based on this model, the slope $1/n$ ranging between 0 and 1 is a measure of surface heterogeneity, becoming more heterogeneous as its value gets closer to zero. A value for $1/n$ below unity indicates a normal Langmuir isotherm, while $1/n$ above one is an indicative of the cooperative adsorption.

Langmuir isotherm [32] is derived from the assumption of monolayer adsorption onto a homogenous surface, with no lateral interaction between the adsorbed molecules. It presumes that adsorption takes place at specific sites within the adsorbent and believes that once the adsorbate occupies a site, no further adsorption could take place at that site. The linear form of Langmuir isotherm is defined as follows:

$$\frac{C_e}{q_e} = \frac{1}{Q_oK_L} + \frac{1}{Q_o}C_e \tag{4}$$

where C_e (mg/L) is the equilibrium concentration of the adsorbate, q_e (mg/g) is the amount of adsorbate

per unit mass of adsorbent, Q_0 and K_L are Langmuir constants related to adsorption capacity and rate of adsorption, respectively. When C_e/q_e is plotted against C_e, a straight line with the slope $1/Q_0$ and the intercept $1/Q_0K_L$ is obtained. The essential characteristics of Langmuir isotherm can be expressed by a dimensionless constant given by:

$$R_L = \frac{1}{1 + K_L C_o} \tag{5}$$

which R_L indicates isotherm to be either unfavorable ($R_L > 1$), linear ($R_L = 1$), favorable ($0 < R_L < 1$) or irreversible ($R_L = 0$).

Whereas Temkin and Pyzhev [33] isotherm is an early model describing the adsorption of hydrogen onto platinum electrodes within the acidic solutions. The isotherm is characterized by a uniform distribution of binding energy and assumes that the heat of adsorption (function of temperature) of all molecules in the layer would decrease linearly rather than logarithmically with surface coverage. Temkin isotherm has been used in the form of:

$$q_e = \left(\frac{RT}{b}\right) \ln (K_T C_e) \tag{6}$$

Eq. (6) can be expressed in its linear form as:

$$q_e = B \ln K_T + B \ln C_e \tag{7}$$

where $RT/b = B$ (J/mol), B is the Temkin constant related to heat of sorption and A (l/g) is the equilib-

Table 1
Langmuir, Freundlich and Temkin isotherm constants for the adsorption of MB onto pineapple leaves derived adsorbent

Langmuir isotherm model	
Q_o (mg/g)	97.09
B (L/mg)	0.074
R^2	0.9952
Freundlich isotherm model	
K_F (mg/g).(L/mg)$^{1/n}$	21.06
n	3.27
R^2	0.9394
Temkin isotherm model	
A (l/g)	1.26
B	17.64
b	142.82
R^2	0.9730

rium binding constant corresponding to the maximum binding energy. R (8.314 J/mol K) is the universal gas constant and T (K) is the absolute temperature.

The isotherm constants determined from the intercept and slope are listed in Table 1. The value of R_L and R^2 in the present investigation has found to be 0.04 and 0.9952, respectively, at 30°C, showing favorable for the adsorption of MB, and applicability of the Langmuir isotherm model. However, the correlation coefficients, R^2 fitted with the Freundlich (0.9394) and Temkin (0.9730) isotherm models were found much lower than the Langmuir isotherm model (0.9952), which ascertained the monolayer coverage of MB onto the prepared adsorbent. Besides it was clearly revealed that increasing concentration from 50 to 300 mg/L demonstrated a gradually decrease of R_L from 0.333 to 0.077, indicating the adsorption process was favorable at the concentrations range being

studied, and higher initial dye concentration which enhances the adsorption process. Table 2 exhibits a comparison of maximum monolayer adsorption capacity of MB onto various adsorbents [34–41]. The adsorbent prepared in this work showed relatively high MB adsorption capacity of 97.09 mg/g, as compared to some previous works as reported in the literature.

3.4. Adsorption kinetics and mechanism

Adsorption kinetics describes the solute uptake rate, which in turn governs residence time and reaction pathways of the adsorption process. When adsorption is preceded by diffusion through a boundary, the kinetics in most systems follow the pseudo-first-order kinetic model. Lagergren [42] proposed pseudo-first-order kinetic equation in the form of:

$$\log\left(\frac{q_e}{q_e - q_t}\right) = \frac{k_1}{2.303} t \qquad (8)$$

where q_e and q_t are the amounts of MB adsorbed (mg/g) at equilibrium and at time t (min), respectively, and k_1 is the pseudo-first-order kinetic rate constant (1/min). The values k_1 and correlation coefficient, R^2 obtained from the plots are summarized in Table 3. The R^2 values which varied from 0.9926 to 0.8051 for the MB initial concentration of 50–300 mg/L were relatively low. Moreover, the experimental q_e values did not agree with the calculated values obtained from the linear plots, suggesting that the adsorption of MB onto the pineapple leaves-based adsorbent did not follow the pseudo-first-order equation.

On the contrary, pseudo-second-order equation [43] predicts the behavior over the whole range of adsorption, with chemisorption being the rate-controlling step. The pseudo-second-order equation based on equilibrium adsorption is expressed as follows:

Table 2
Comparison of adsorption capacities of various adsorbents for MB

Adsorbent	Q_0 (mg/g)	T (°C)	References
Waste pineapple leaves	109.89	30	Present study
Yellow passion fruit peel	0.0068	25	[34]
Firwood activated carbon	1.21	30	[35]
Activated clay	127.50	30	[36]
Tea waste	85.16	27	[37]
Coal fly ash	12.70	30	[38]
Coarse grinded wheat straw	3.82	30	[39]
Coffee husks	90.10	30	[40]
Posidonia oceanica (L.) fibres	5.56	30	[41]

Table 3
Kinetic models parameters for the adsorption of MB onto pineapple leaves derived adsorbent at different initial MB concentrations

C_o (mg/L)	$q_{e,\ exp}$ (mg/g)	Pseudo-first-order kinetic model			Pseudo-second-order kinetic model			
		$q_{e1,\ cal}$ (mg/g)	k_1 (1/min)10^{-1}	R^2	$q_{e2,\ cal}$ (mg/g)	k_2 (g/mg min)10^{-3}	R^2	h (mg/g min)
50	31.81	25.12	0.08	0.9607	36.23	0.39	0.9969	0.52
100	55.18	54.63	0.10	0.9926	65.79	0.19	0.9967	0.82
150	74.93	80.52	0.11	0.9793	89.29	0.14	0.9915	1.12
200	80.69	82.39	0.12	0.9887	92.59	0.17	0.9971	1.46
250	85.01	122.66	0.17	0.8051	96.15	0.20	0.9976	1.85
300	94.97	82.68	0.12	0.9724	104.17	0.22	0.9992	2.39

$$\frac{t}{q_t} = \frac{1}{k_2 q_e^2} + \frac{1}{q_e} t \qquad (9)$$

where k_2 (g/mg h) is the pseudo-second-order kinetic rate constant. The result revealed good agreement between the experimental and the calculated q_e values (Table 3). Besides, the correlation coefficients for the second-order kinetic model were greater than 0.99 for all MB concentrations, indicating applicability of the second-order kinetic model to describe the sorption process.

The adsorption mechanism was further analyzed using the Webber and Morris [44] intraparticle diffusion model. According to the theory:

$$q_t = k_{id} t^{1/2} + C \qquad (10)$$

where C is the intercept and k_{id} is the intraparticle diffusion rate constant (mg/g min$^{0.5}$), which can be evaluated from the slope of the linear plots of q_t vs. $t^{1/2}$ (Fig. 3). The first sharper portion is related to the diffusion of adsorbate through solution to the external surface of adsorbent (external surface adsorption). The second portion describes the gradual layer adsorption stage, where intraparticle diffusion is rate-limiting and the third portion is the final equilibrium stage, where intraparticle diffusion started to slow down due to extremely low adsorbate concentrations left in the solution.

As clearly shown in graphical plots in Fig. 3, the linear lines of the second and third stages did not pass through the origin, due to the difference in the mass transfer in the initial and final stages of adsorption. The deviation also illustrated the presence of multilinearity [45]. This implied that intraparticle diffusion was not the only rate limiting mechanism in the adsorption process. Increasing bulk liquid dye

concentrations from 50 to 300 mg/L showed an enhancement of pore diffusion rate and intercept, indicative of the increase in thickness of the boundary layer and driving force for the sorption process.

3.5. Characterization of the prepared adsorbent

Fig. 4 illustrates the SEM of the pineapple leaves derived adsorbent before and after the adsorption of MB. It can be clearly seen that the adsorbent surface exhibits an even and heterogeneous structure (Fig. 4(a)), indicating good possibility for the dyes to be trapped and adsorbed. However, the surface of the dye-loaded adsorbent displays a rougher texture, covered with the adsorbed MB dye molecules (Fig. 4(b)). The obtained FTIR spectrum of pineapple leaves derived adsorbent

(a)

(b)

Fig. 4. SEM micrograph for pineapple leaves derived adsorbent (a) before (150×) and (b) after the adsorption process (150×).
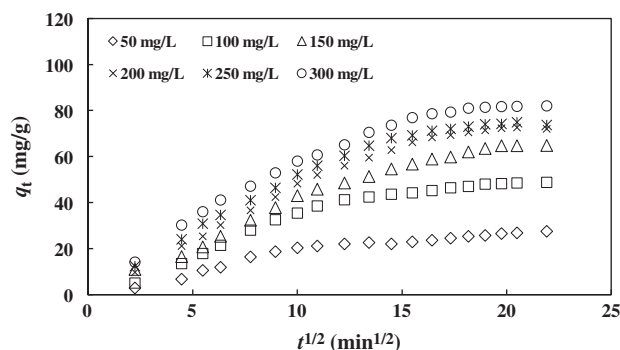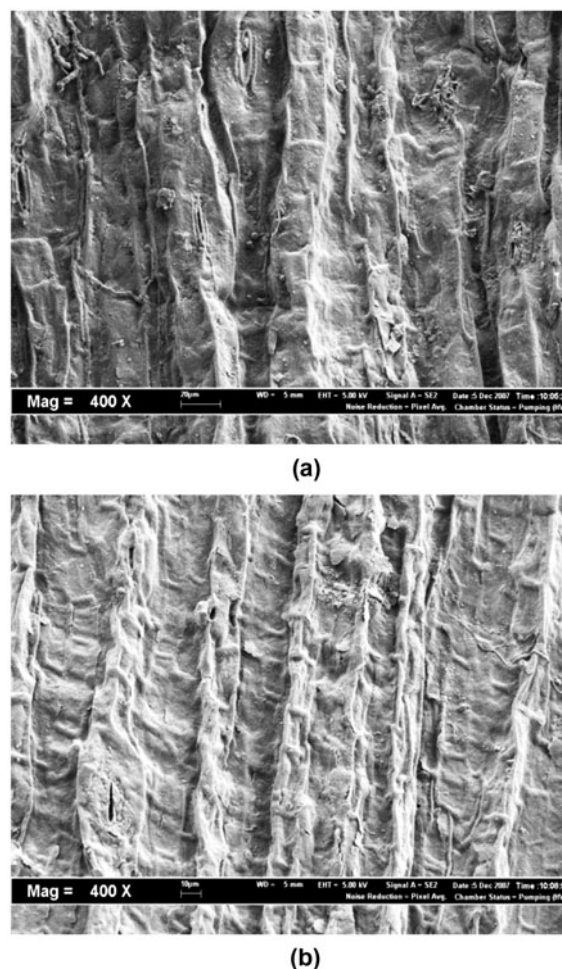

Fig. 3. Plots of intraparticle diffusion model for the adsorption of MB onto pineapple leaves derived adsorbent for different initial MB concentrations at 30℃.

Table 4
FTIR of the adsorbent: (a) before and (b) after the adsorption of MB

IR peak	Before adsorption	After adsorption	Assignment
1	3,399	3,402	Bonded –OH groups
2	2,918	2,127	Two bands for $-CH_2-$ groups
3	2,125	–	C=N stretching
4	1,736	1,739	C=O stretching
5	1,644	–	C=O stretching
6	1,515	1,518	Bonded C=C
7	1,427	–	NH stretching
8	1,377	–	In-plane −OH bending and C–O stretch of dimmers
9	1,318	1,310	CH_3 deformation
10	1,251	1,130	$-NO_2$ aromatic nitro compounds
11	1,162	–	SO_2-NH_2 sulfonamides
12	1,105	1,060	C–O stretching
13	1,056	899	C–N stretching
14	899	909	$-C-NH_3$ primary aliphatic amines
15	830, 800	–	P–O–C strongest band highest frequencies for aliphatic amines
16	775, 746	–	CH out-of-plane deformation
17	721, 700	–	CH out-of-plane deformation
18	672, 621	–	C–O–H twist broad

(Table 4) revealed the peaks at 3,399, 2,918, 2,125, 1,736, 1,515, 1,427, 1,377, 1,318, 1,251, 1,162, 1,105, 1,056, 899, 830, 775, 721, and $672 \, cm^{-1}$ corresponded to the presence of –OH, $-CH_2-$, C=N, C=O, C=C, NH, C–O, CH_3, $-NO_2$ aromatic nitro, SO_2-NH_2 sulfonamides, C–O, C–N, $-C-NH_3$, P–O–C, CH, and C–O–H functional groups. Meanwhile, the adsorbent detected some shift, disappear and new peaks after the adsorption of MB, elucidating possible involvement of the functional groups during the adsorption process.

4. Conclusion

The present study investigated the versatility of pineapple waste developed adsorbent for removing MB dye from the aqueous solutions. Adsorption equilibrium increased with increasing the contact time, initial MB concentration, and solution pH. Experimental data were best described by the Langmuir isotherm models, with a maximum monolayer adsorption capacity of 97.09 mg/g at 30°C. Kinetics study was well fitted to the pseudo-second-order kinetic model, suggesting a chemisorption process.

References

[1] F.A. Nasr, A.M. Ashmawy, H.S. Ibrahim, M.A. El-Khateeb, Management of wastewater from ink production and metal plating industries in an Egyptian industrial city, Desalin. Water Treat. 21 (2010) 8–16.

[2] K.Y. Foo, B.H. Hameed, An overview of dye removal via activated carbon adsorption process, Desalin. Water Treat. 19 (2010) 255–274.

[3] V.K.G. Suhas, Application of low-cost adsorbents for dye removal—A review, J. Environ. Manage. 90 (2009) 2313–2342.

[4] A. Ojstrsek, D. Fakin, Colour and TOC reduction using biofilter packed with natural zeolite for the treatment of textile wastewaters, Desalin. Water Treat. 33 (2011) 147–155.

[5] R.G. Saratale, G.D. Saratale, J.S. Chang, S.P. Govindwar, Bacterial decolorization and degradation of azo dyes: A review, J. Taiwan Inst. Chem. Eng. 42 (2011) 138–157.

[6] C. Meziti, A. Boukerroui, Removal of a basic textile dye from aqueous solution by adsorption on regenerated clay, Procedia Eng. 33 (2012) 303–312.

[7] S.K.A. Solmaz, G.E. Ustun, F. Ciner, Treatability of organized industrial district (OID) effluent for reuse in agriculture, Desalin. Water Treat. 33 (2011) 156–163.

[8] R. Schurer, A. Janssen, L.O. Villacort, M. Kennedy, Performance of ultrafiltration and coagulation in an UF-RO seawater desalination demonstration plant, Desalin. Water Treat. 42 (2012) 57–64.

[9] J. Nan, W.P. He, Characteristic analysis on morphological evolution of suspended particles in water during dynamic flocculation process, Desalin. Water Treat. 41 (2012) 35–44.

[10] M. Sivanatham, B.V.R. Tata, C.A. Babu, Synthesis of crown ether functionalized polyacrylamide gel beads and their extraction behaviour for strontium ions, Desalin. Water Treat. 38 (2012) 8–14.

[11] D.S. Filho, G.B. Bota, R.B. Borri, F.J.C. Teran, Electrocoagulation/floatation followed by fluidized bed anaerobic reactor applied to tannery effluent treatment, Desalin. Water Treat. 37 (2012) 359–363.

[12] T. Meyn, J. Altmann, T. Leiknes, In-line coagulation prior to ceramic microfiltration for surface water treatment—minimisation of flocculation pre-treatment, Desalin. Water Treat. 42 (2012) 163–176.

[13] A. Lerch, N. Siebdrath, P. Berg, V. Gitis, W. Uhl, Fouling minimised reclamation of secondary effluents with reverse osmosis (ReSeRO), Desalin. Water Treat. 42 (2012) 181–188.

[14] I. Zaslavschi, D. Hasson, H. Shemer, R. Semiat, M. Wilf, C. Bartels, Correlation of CaCO$_3$ induction times measured by an electrochemical technique, Desalin. Water Treat. 31 (2011) 59–63.

[15] H.Q. Chu, Y.L. Zhang, B.Z. Dong, X.F. Zhou, D.W. Cao, Z.M. Qiang, Z.X. Yu, H.W. Wang, Pretreatment of micro-polluted surface water with a biologically enhanced PAC–diatomite dynamic membrane reactor to produce drinking water, Desalin. Water Treat. 40 (2012) 84–91.

[16] J.F. Sempere, F.R. Bevia, R.S. Diaz, P.G. Algado, M.G. Rodriguez, Digital holographic interferometry visualization of PEG-10000 accumulation on an acetate cellulose membrane: Assessment of polarization layer and adsorption phenomenon, Desalin. Water Treat. 42 (2012) 49–56.

[17] K.Y. Foo, B.H. Hameed, Potential of activated carbon adsorption processes for the remediation of nuclear effluents: A recent literature, Desalin. Water Treat. 41 (2012) 72–78.

[18] C. Hua, R.H. Zhang, L. Li, X.Y. Zheng, Adsorption of phenol from aqueous solutions using activated carbon prepared from crofton weed, Desalin. Water Treat. 37 (2012) 230–237.

[19] J. Morton, Pineapple, in: J.F. Morton (Ed.), Fruits of Warm Climates, Creative Resource Systems, Miami, FL, 1987, pp. 18–28.

[20] K.Y. Foo, B.H. Hameed, Porous structure and adsorptive properties of pineapple peel based activated carbons prepared via microwave assisted KOH and K$_2$CO$_3$ activation, Micropor. Mesopor. Mater. 148 (2012) 191–195.

[21] A.H. Sulaymon, S.E. Ebrahim, Saving amberlite XAD4 by using inert material in adsorption process, Desalin. Water Treat. 20 (2012) 234–242.

[22] Q. Zhou, W.Q. Gong, C.X. Xie, Y.B. Li, C.P. Bai, S.H. Chen, Biosorption of methylene blue from aqueous solution on spent cottonseed hull substrate for *Pleurotus ostreatus* cultivation, Desal. Wat. Treat. 29 (2011) 317–325.

[23] J.Q. Liang, J.H. Wu, P. Li, X.D. Wang, B. Yang, Shaddock peel as a novel low-cost adsorbent for removal of methylene blue from dye wastewater, Desalin. Water Treat. 39 (2012) 70–75.

[24] F.C.C. Assis, S. Albeniz, A. Gil, S.A. Korili, R. Trujillano, M.A. Vicente, L. Marcal, M. Saltarelli, K.J. Ciuffi, Removal of organic pollutants from industrial wastewater-performance evaluation of inorganic adsorbents based on pillared clays, Desalin. Water Treat. 39 (2012) 316–322.

[25] X.L. Han, W. Wang, X.J. Ma, Adsorption characteristics of methylene blue onto low cost biomass material lotus leaf, Chem. Eng. J. 171 (2011) 1–8.

[26] R.P. Han, J.J. Zhang, P. Han, Y.F. Wang, Z.H. Zhao, M.S. Tang, Study of equilibrium, kinetic and thermodynamic parameters about methylene blue adsorption onto natural zeolite, Chem. Eng. J. 145 (2009) 496–504.

[27] M.C. Shih, Kinetics of the batch adsorption of methylene blue from aqueous solutions onto rice husk, effect of acid-modified process and dye concentration, Desalin. Water Treat. 37 (2012) 200–214.

[28] X.Z. Bu, G.K. Zhang, Y.D. Guo, Thermal modified palygorskite: Preparation, characterization, and application for dye-containing wastewater purification, Desalin. Water Treat. 30 (2011) 339–347.

[29] A.E. Ofomaja, Equilibrium sorption of methylene blue using mansonia wood sawdust as biosorbent, Desalin. Water Treat. 3 (2009) 1–10.

[30] K. Mahmud, M.A. Islam, A. Mitsionis, T. Albanis, T. Vaimakis, Adsorption of direct yellow 27 from water by poorly crystalline hydroxyapatite prepared via precipitation method, Desalin. Water Treat. 41 (2012) 170–178.

[31] H. Freundlich, Über dye adsorption in lösungen (adsorption in solution), Z. Phys. Chem. 57 (1906) 384–470.

[32] I. Langmuir, The adsorption of gases on plane surfaces of glass, mica and platinum, J. Am. Chem. 57 (1918) 1361–1403.

[33] M.I. Temkin, V. Pyzhev, Kinetics of ammonia synthesis on promoted iron catalyst, Acta Phys. Chim. USSR 12 (1940) 327–356.

[34] F.A. Pavan, A.C. Mazzocato, Y. Gushiken, Removal of Methylene blue dye from aqueous solutions by adsorption using yellow passion fruit peel as adsorbent, Bioresour. Technol. 99 (2008) 3162–3165.

[35] F.C. Wu, R.L. Tseng, High adsorption capacity NaOH-activated carbon for dye removal from aqueous solution, J. Hazard. Mater. 152 (2008) 1256–1267.

[36] C.H. Weng, Y.F. Pan, Adsorption of a cationic dye (methyleneblue) onto spent activated clay, J. Hazard. Mater. 144 (2007) 355–362.

[37] M.T. Uddin, M.A. Islam, S. Mahmud, M. Rukanuzzaman, Adsorptive removal of methylene blue by tea waste, J. Hazard. Mater. 164 (2009) 53–60.

[38] S. Wang, Q. Ma, Z.H. Zhu, Characteristics of coal fly ash and adsorption application, Fuel 87 (2008) 3469–3473.

[39] F.A. Batzias, D.K. Sidiras, E. Schroeder, C. Weber, Simulation of dye adsorption on hydrolyzed wheat straw in batch and fixed-bed systems, Chem. Eng. J. 148 (2009) 459–472.

[40] L.S. Oliveira, A.S. Franca, T.M. Alves, S.D.F. Rocha, Evaluation of untreated coffee husks as potential biosorbents for treatment of dye contaminated waters, J. Hazard. Mater. 155 (2008) 507–512.

[41] M.C. Ncibi, A.M.B. Hamissa, A. Fathallah, M.H. Kortas, T. Baklouti, B. Mahjoub, M. Seffen, Biosorptive uptake of methyleneblue using Mediterranean green alga Enteromorpha spp, J. Hazard. Mater. 170 (2009) 1050–1055.

[42] S. Langergren, About the theory of so-called adsorption of soluble substances, Kungliga Svenska Vetenskapsakademies Handlingar 24 (1898) 1–39.

[43] Y.S. Ho, G. McKay, Sorption of dye from aqueous solution by peat, Chem. Eng. J. 70 (1998) 115–124.

[44] W.J.J. Weber, J.C. Morris, Kinetics of adsorption on carbon from solution, J. Sanitary Eng. Div. Am. Soc. Civ. Eng. 89 (1963) 31–60.

[45] V.J.P. Poots, G. McKay, J.J. Healy, The removal of acid dye from effluent using natural adsorbents: I Peat, Water Res. 10 (1976) 1061–1066.